



# Single Sneutrino/Slepton Production at LEP2 and the NLC

B.C. Allanach<sup>1</sup>, H. Dreiner<sup>1</sup>, P. Morawitz<sup>2</sup> and M.D. Williams<sup>2</sup>

<sup>1</sup> Rutherford Lab., Chilton, Didcot, OX11 0QX, UK

<sup>2</sup> Imperial College, HEP Group, London SW7 2BZ, UK

## Abstract

We propose a new method of detecting supersymmetry at LEP2 and the NLC when R-parity is violated by an  $LL\bar{E}$  operator. We consider the processes  $e\gamma \rightarrow \tilde{\nu}_j e_k$  and  $e\gamma \rightarrow \tilde{l}_k \bar{\nu}_j$  which can test seven of the nine  $LL\bar{E}$ -operators. A Monte-Carlo analysis is performed to investigate the sensitivity to the sneutrino signal, and the  $5\sigma$  discovery contours in the  $m_{\tilde{\nu}_j}$  vs.  $\lambda$  plane are presented. For an integrated luminosity of  $100 \text{ pb}^{-1}$ , sneutrinos with masses up to  $M_{\tilde{\nu}} < 170 \text{ GeV}/c^2$  could be discovered in the near future at LEP2. For the charged slepton production the cross-section is too low to be detectable.

## 1 Introduction

In the R-parity violating version of the minimal supersymmetric standard model [1] supersymmetric particles can be produced singly. The production cross section is suppressed by the  $\tilde{A}_p$  Yukawa coupling but the kinematic reach is typically twice that of supersymmetric pair production mechanism. Here, we consider the possible detection of R-parity violating supersymmetry at LEP2 through the superpotential terms<sup>1</sup>

$$W_{LLE} = \frac{1}{2} \lambda_{ijk} (\epsilon_{\alpha\beta} L_i^\alpha L_j^\beta) E_k^c, \quad (1)$$

where  $i, j, k = 1, 2, 3$  are family indices and  $\alpha, \beta = 1, 2$  are  $SU(2)$ -gauge indices.  $\epsilon_{\alpha\beta}$  is the totally antisymmetric tensor,  $\epsilon_{12} = +1$ .

The single *resonant* production of sneutrinos at  $e^+e^-$ -colliders was first considered in [2, 3]. More detailed studies for specific colliders (LEP2, NLC) were

---

<sup>1</sup>Here  $L$  and  $E$  are the  $SU(2)$  doublet and singlet lepton superfields respectively.

performed in [4] and experimental analyses have since been performed [5]. All of these studies were based on the assumption of a single dominant coupling. If this assumption is dropped the resonantly produced sneutrino can also decay via other non-vanishing operators [6, 7]. All of these previous studies were restricted to the operators  $L_1 L_{2,3} \bar{E}_1$ . In [7] the indirect effects of the t-channel exchange of a sneutrino were studied for dominant  $L_1 L_{2,3} \bar{E}_1$ , as well. This could easily be extended to other operators  $LLE^c$ . However, the effect is too small to be relevant.

None of the previous direct searches considered the operators

$$L_1 L_2 E_2^c, L_1 L_2 E_3^c, L_1 L_3 E_2^c, L_1 L_3 E_3^c, L_2 L_3 E_1^c, \quad (2)$$

as well as  $L_2 L_3 \bar{E}_{2,3}$ . In this letter we investigate the possibility of directly testing the operators (2) via sneutrino or slepton production

$$\gamma(p_1) + e^\pm(p_2) \rightarrow e_k^\pm(q_1) + \tilde{\nu}_j(q_2), \quad (3)$$

$$\gamma(p_1) + e^\pm(p_2) \rightarrow \tilde{e}_j^\pm(q_1) + \nu_k(q_2). \quad (4)$$

In parentheses we have included the 4-momenta used in the calculation below. These processes are competitive for  $e_k = \mu, \tau$  and  $\tilde{\nu}_j = \tilde{\nu}_\mu, \tilde{\nu}_\tau$ . Due to the incoming photon we are only restricted to one electron index. The final state charged lepton/slepton can be an SU(2) doublet or an SU(2) singlet. The indices  $j, k = 1, 2, 3$  are free. Thus we can in principle also study the operators  $L_1 L_{2,3} E_1^c$  but here the resonant sneutrino production is more sensitive. For simplicity we shall only consider one non-zero  $\mathcal{R}_p$  coupling at a time. The operators  $LLE^c$  can also be tested at hadron colliders via various direct and indirect signatures [8].

## 2 Cross Section Evaluation

The tree-level Feynman diagrams for the sneutrino production (3) are shown in Figure 1. The spin averaged matrix element squared for this process in the Weizsäcker-Williams approximation [9] (on-shell photon) is given by<sup>2</sup>

$$|\bar{M}|^2 = e^2 \lambda^2 \left[ \frac{u'(t' - 3m_{e_k}^2)}{s'(t' - m_{e_k}^2)} + \frac{3m_{e_k}^4 - t'^2 + 2u'^2}{2s'(t' - m_{e_k}^2)} + \frac{8m_{e_k}^4 + t'(2t' + 2u' - s') - m_{e_k}^2(5s' + 4t' + 8u')}{2(t' - m_{e_k}^2)^2} \right]. \quad (5)$$

The symbol  $e$  denotes the absolute value of the charge of the electron and  $\lambda$  is the  $\mathcal{R}_p$  Yukawa coupling.  $m_{e_k}$  is the mass of the charged lepton  $e_k$  and we

<sup>2</sup>This matrix element squared was first presented in [10] in the limit of a massless final state charged lepton  $m_{e_k} = 0$ .

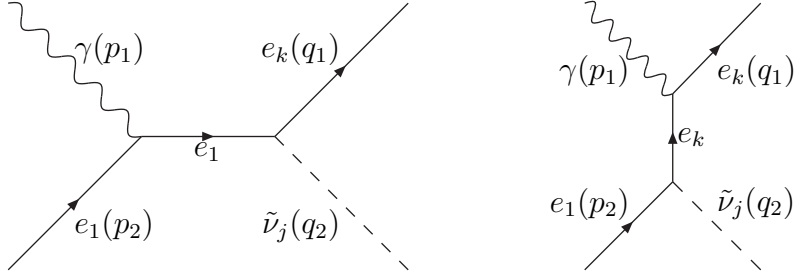


Figure 1: Feynman diagrams contributing to the  $\gamma e \rightarrow e_k \tilde{\nu}$  sub-process.

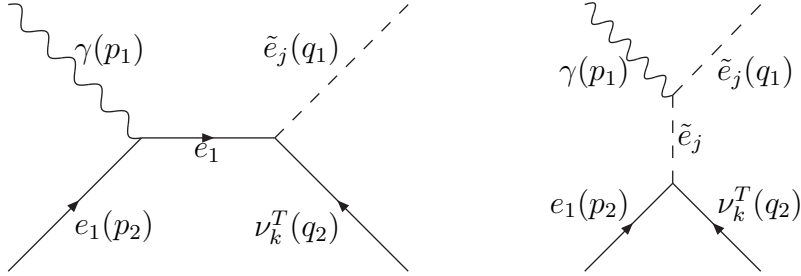


Figure 2: Feynman diagrams contributing to the  $\gamma e \rightarrow \tilde{e}_j \nu_k$  subprocess. Arrows on fermion lines denote flow of fermion number not momentum.

have neglected the mass of the incoming electron. We have made use of the Mandelstam variables

$$\begin{aligned}
 s' &= (p_1 + p_2)^2 = 2p_1 \cdot p_2, \\
 t' &= (p_1 - q_1)^2 = -2p_1 \cdot q_1 + m_{e_k}^2, \\
 u' &= (p_1 - q_2)^2 = -2p_1 \cdot q_2 + m_{\tilde{\nu}}^2,
 \end{aligned} \tag{6}$$

where  $m_{\tilde{\nu}}$  is the mass of the produced sneutrino and the four-momenta are defined in Eq.(3) and Figure 1.

The tree-level diagrams for the selectron production (4) are shown in Figure 2. The spin-averaged matrix-element squared is given in the Weizsäcker-Williams approximation [9] by

$$|\bar{M}|^2 = \frac{e^2 \lambda^2}{2} \left[ \frac{t''(t'' + m_{\tilde{e}}^2)}{(t'' - m_{\tilde{e}}^2)^2} - \frac{u''}{s''} + \frac{t''(2m_{\tilde{e}}^2 - s'')}{s''(t'' - m_{\tilde{e}}^2)} \right], \tag{7}$$

where  $m_{\tilde{e}}$  is the mass of the produced selectron. We have neglected the electron mass. The Mandelstam variables are as in Eqs.(6) with the replacements  $(s', t', u') \rightarrow (s'', t'', u'')$  combined with  $m_{\tilde{\nu}} \rightarrow 0$ ,  $m_{e_k} \rightarrow m_{\tilde{e}}$ .

The total cross-section for the  $e\gamma$  subprocesses may be written as

$$\sigma(s'; e\gamma) = \int_{t_{min}}^{t_{max}} \frac{1}{16\pi s'^2} |\bar{M}|^2 dt, \tag{8}$$

where

$$t_{max/min} = \left( \frac{m_{q_2}^2 - m_{q_1}^2}{2\sqrt{s'}} \right)^2 - \left( \frac{\sqrt{s'}}{2} \mp \sqrt{\left( \frac{s' + m_{q_1}^2 - m_{q_2}^2}{2\sqrt{s'}} \right)^2 - m_{q_1}^2} \right)^2, \quad (9)$$

where  $m_{q_1}$  and  $m_{q_2}$  are the masses of the particles with momenta  $q_1$  and  $q_2$ , and the variable  $s'$  (or  $s''$  for selectrons) is defined in Eqs.(6). The cross-sections for  $e^+e^- \rightarrow e\tilde{\nu}$  and  $e^+e^- \rightarrow e\tilde{\ell}$  are obtained from the  $e\gamma$  cross-section by

$$\sigma(s; e^+e^-) = 2 \int_0^1 f_\gamma(y) \sigma(ys; e\gamma) dy, \quad (10)$$

where  $f_\gamma(y)$  is the photon distribution in the electron at a given fraction,  $y$ , of the electron momentum. The factor of two is due to the charge conjugate diagrams when an anti-sneutrino or anti-charged slepton is produced. We use the following version of the Weizsäcker-Williams distribution [11]:

$$f_\gamma(y) = \frac{\alpha_{em}}{2\pi} \left\{ 2(1-y) \left[ \frac{m_e^2 y}{E^2(1-y)^2\theta_c^2 + m_e^2 y^2} - \frac{1}{y} \right] + \frac{1+(1-y)^2}{y} \log \frac{E^2(1-y)^2\theta_c^2 + m_e^2 y^2}{m_e^2 y^2} \right\}, \quad (11)$$

where  $\theta_c$  is the maximum scattering angle of the beam electron and  $E$  is the beam energy. The value of  $\theta_c$  is taken to be 30 mrad - a typical value for the coverage of the luminosity monitors in the LEP experiments - for two reasons: Firstly because for large values of  $\theta_c$  the photon emitted from the beam electron is no longer on-shell, and the validity of the Weizsäcker-Williams approximation is compromised. And secondly because it simplifies the feasibility study presented in Section 3, which considers three lepton topologies, assuming that the beam electron deflected at small angles is not measured in the detector. If we were to allow for the full range of  $\theta_c$  in Eq.(11), the cross-section would be larger by approximately 20%. The cross-sections for  $e^+e^- \rightarrow e\mu\tilde{\nu}$  and  $e^+e^- \rightarrow e\tau\tilde{\nu}$  are shown as a function of the slepton and sneutrino mass in Figure 3 for  $\lambda_{ijk} = 0.05$ . The cross-section for single slepton production is much smaller than that for single sneutrino production, since the t-channel diagram (which is the dominant diagram) is suppressed. Single selectron production is unlikely to be detectable for any reasonable expected luminosity at LEP2, and we consequently neglect this possibility from now on. We also present, in Figure 4, the single sneutrino production cross-section at a Next Linear Collider operating at a centre of mass energy of 500 GeV.

### 3 Single Sneutrino Production

The signal  $e^+e^- \rightarrow e\tilde{\nu}$  is characterised by the electron continuing along the beam pipe, so that the only particles visible in the detector are the charged lepton  $\ell$

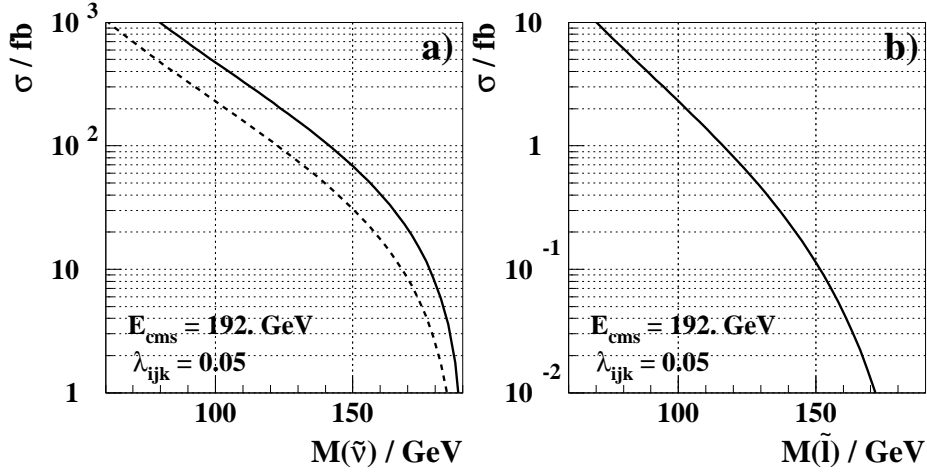


Figure 3: The cross-sections for single production of a) sneutrinos and b) charged sleptons at a centre-of-mass energy of 192 GeV and for  $\lambda_{ijk} = 0.05$  as a function of the sneutrino/slepton mass. In a) the solid line is the cross-section for  $e^+e^- \rightarrow e\mu\tilde{\nu}$  and the dashed line is the cross-section for  $e^+e^- \rightarrow e\tau\tilde{\nu}$ .

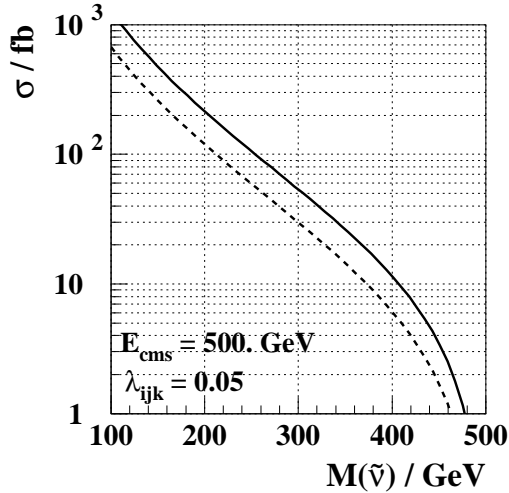


Figure 4: The cross-section for single production of sneutrinos at a Next Linear Collider with a centre-of-mass energy of 500 GeV as a function of the sneutrino mass. The solid line is the cross-section for  $e^+e^- \rightarrow e\mu\tilde{\nu}$  and the dashed line is the cross-section for  $e^+e^- \rightarrow e\tau\tilde{\nu}$ .

Coupling	Direct Decays		Indirect Decays	
	$\tilde{\nu}_\mu$	$\tilde{\nu}_\tau$	$\tilde{\nu}_\mu$	$\tilde{\nu}_\tau$
122	$e\mu^+\mu^-$	-	$\mu\nu\chi$	-
123	$e\tau^+\tau^-$	-	$\tau\nu\chi$	-
132	-	$e\mu^+\mu^-$	-	$\mu\nu\chi$
133	-	$e\tau^+\tau^-$	-	$\tau\nu\chi$
231	$e\tau^+\tau^-$	$e\mu^+\mu^-$	$\tau\nu\chi$	$\mu\nu\chi$

Table 1: The final states for production of different sneutrino flavours via different couplings for the *direct* decays and the *indirect* decays to the lightest neutralino. The entries marked with a dash are those for which that sneutrino flavour cannot be produced by the coupling in question.

and the decay products of the sneutrino. The sneutrino can either decay *directly*,  $\tilde{\nu} \rightarrow e\ell$ , or *indirectly* via lighter neutralinos or charginos, eg.  $\tilde{\nu} \rightarrow \nu\chi^0, \ell^-\chi^+$ . In the following analysis we only consider the direct decays and the indirect decays to neutralinos for simplicity. The final state depends upon both the coupling involved and the flavour of sneutrino produced. This information is summarised in Table 1.

For a coupling  $\lambda_{ijk}$  the lightest neutralino can decay to the following final states:

$$\tilde{\chi}_1^0 \rightarrow \left\{ l_i^- \bar{\nu}_j l_k^+, l_i^+ \nu_j l_k^-, \bar{\nu}_i l_j^- l_k^+, \nu_i l_j^+ l_k^- \right\}. \quad (12)$$

Thus the signal for sneutrino production followed by an indirect decay to the lightest neutralino contains three charged leptons and two neutrinos. The latter contributes substantial missing transverse momentum.

To investigate the viability of searching for these signals we have written a Monte Carlo capable of generating the different final states and included an interface to JETSET [12] for the decays and to PHOTOS [13] for final state radiation. Several simple analyses to discriminate the signal from the dominant backgrounds were developed. PHOT02 [14] was used to generate tagged  $\gamma\gamma \rightarrow \mu^+\mu^-$  and untagged  $\gamma\gamma \rightarrow \tau^+\tau^-$  and PYTHIA [12] to generate  $Zee, W\ell\nu, ZZ$  and  $W^+W^-$ . Two photon processes and  $Zee$  are the most important backgrounds. No attempt was made to include the effects of detector performance, but the acceptance of a typical LEP experiment was accounted for in the following simple manner. The energy of a particle was assumed to be detected if the particle had a polar angle greater than 30 mrad from the beam axis. Charged particles were assumed to be tracked over the polar angle range  $|\cos\theta| < 0.95$  and electrons and muons were only allowed to be identified as such if they fell within this range.

For the direct decays two analyses were developed to search for decays to  $e\mu$  and to  $e\tau$ . Similarly, two analyses were developed for the best ( $\lambda_{122}$ ) and worst ( $\lambda_{133}$ ) case indirect decays. These are summarised in Table 2.

Direct  $\mathcal{R}_p$  sneutrino decays have a similar signature to  $\gamma\gamma \rightarrow \mu\mu$  or  $\tau\tau$  with a

	Direct $e\mu$	Direct $e\tau$	Indirect $\lambda_{122}$	Indirect $\lambda_{133}$
Cuts	$N_{ch} = 3$ $2\mu + 1e$ $\langle p_T \rangle > 15 \text{ GeV}$ $ \cos \phi_e  < 0.8$ $M_{vis} > 80 \text{ GeV}$ $M_{\tilde{\nu}} > 60 \text{ GeV}$	$N_{ch} = 3 \text{ or } 5$ $N_e = 1 \text{ or } 2$ $\langle p_T \rangle > 15 \text{ GeV}$ $ \cos \phi_e  < 0.8$ $p'_T > 10 \text{ GeV}$	$N_{ch} = 3$ $N_e + N_\mu = 3$ $p'_T > 10 \text{ GeV}$ $ \cos \theta_m  < 0.95$	$N_{ch} = 3 \text{ or } 5$ $N_e + N_\mu \geq 1$ $p'_T > 10 \text{ GeV}$ $ \cos \theta_m  < 0.95$ $5 < M_{vis} < 60$ $E_{ch} < 70 \text{ GeV}$
Bkgrd.	27 fb	36 fb	12 fb	21 fb
Eff.	45%	43%	49%	42%

Table 2: Summary of the simple analyses used to derive the possible discovery limits. The efficiencies for a 100 GeV sneutrino are also shown. For the case of the indirect decays the efficiency assumes a neutralino of 50 GeV.

single tagged beam electron. In the case of the signal, the electron is produced from the decay of a massive sneutrino and is typically emitted with a large angle,  $\phi_e$ , with respect to the beam axis. In addition, the average transverse momentum of the charged tracks,  $\langle p_T \rangle$ , is larger than for a typical  $\gamma\gamma$  event. For the direct decays to  $e\mu$  a large visible mass is required and the invariant mass of the sneutrino,  $m_{\tilde{\nu}}$ , can easily be constructed. Only values of  $m_{\tilde{\nu}} > 60 \text{ GeV}/c^2$  that are not already excluded [15] are considered. It would be possible to use the distribution of  $m_{\tilde{\nu}}$  to improve the sensitivity to the signal. This distribution is shown in Figure 5 for a sneutrino mass of 100 GeV and a coupling of  $\lambda = 0.05$ , assuming an invariant mass resolution of 2.5 GeV. The signal peak is clearly visible above the background. Large missing transverse momentum,  $p'_T$ , is required for the direct decays to  $e\tau$ .

For the indirect decays via a single neutralino substantial missing energy is expected because of the presence of an energetic neutrino. This neutrino also means that the polar angle of the missing momentum,  $\theta_m$ , is not generally along the beam direction. The decay products of the neutralino depend upon the choice of coupling. For a  $\lambda_{122}$  coupling there are three charged leptons in the event and this can be used to reduce the background. For a  $\lambda_{133}$  coupling the visible mass and total charged energy are required to be small. The analyses, the remaining backgrounds and the efficiencies to select a signal of a sneutrino of 100 GeV and, for the indirect decays, a neutralino of 50 GeV are shown in Table 2. The best performance is achieved for the indirect decays and a coupling  $\lambda_{122}$ ; the analysis for direct decays to  $e\tau$  has the worst performance due to the larger background.

Using these simple selection criteria and parameterising the variation of the efficiency with sneutrino mass we can derive expected  $5\sigma$  discovery contours in the  $(m_{\tilde{\nu}}, \lambda)$ -plane. The discovery criterion is defined as follows: For a number of signal events,  $S$ , and background events,  $B$ , we find  $S$  such that the probability that the background fluctuates to  $S + B$  or more is less than  $5.7 \times 10^{-5}$ , i.e.  $5\sigma$  from the



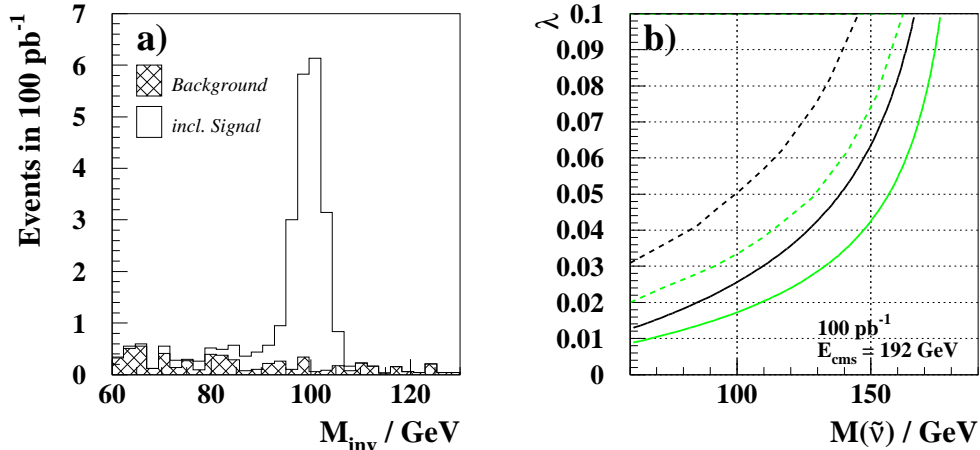


Figure 5: a) shows the distribution of the invariant mass of the electron and muon from a sneutrino decay with  $M_{\tilde{\nu}} = 100$  GeV, compared to the expectation from the combined backgrounds for an integrated luminosity of  $100 \text{ pb}^{-1}$  and a coupling of  $\lambda = 0.05$ . In b) the discovery contours are shown in the  $(m_{\tilde{\nu}}, \lambda)$  plane. The solid lines are for the best case (indirect decays with  $\lambda_{122}$ ) and the dashed are for the worst case (direct decays to  $e\tau$ ). The black lines correspond to a single experiment and the grey lines are for a combination of all four LEP experiments.

expectation. In Figure 5 these contours are shown assuming  $100 \text{ pb}^{-1}$  of data are collected at a centre of mass energy of  $192 \text{ GeV}$ . Much better performance could be obtained for the case of direct decays to  $e\mu$  by including the mass distribution of the events. These results should be compared with the available limits upon  $\mathcal{R}_p$ -couplings. The best current limits on  $\lambda_{ijk}$  in Eq.1 are<sup>3</sup> [16]

$$\lambda_{12n} < 0.05 \quad \lambda_{131} < 0.04 \quad \lambda_{132} < 0.04 \quad \lambda_{133} < 0.004 \quad \lambda_{23n} < 0.05, \quad (13)$$

for the right-handed selectron mass of the third index in  $\lambda_{ijk}$   $\tilde{m}_{e_k^c} = 100 \text{ GeV}$ . (The bounds directly depending on the sneutrino mass are weaker.) All but the specific bound on  $\lambda_{133}$  scale as  $(m_{\tilde{e}_k^c}/100 \text{ GeV})$ . If we compare these bounds with the results presented in Figure 5 we see that there is a substantial discovery potential for this new process.

## 4 Conclusion

We have calculated the matrix elements for  $e\gamma \rightarrow \tilde{\nu}_j e_k$  and  $e\gamma \rightarrow \tilde{l}_k \bar{\nu}_j$  via an R-parity violating coupling of type  $LL\bar{E}$  and obtained the cross-sections in  $e^+e^-$

<sup>3</sup>The bounds on  $\lambda_{12n}$  are at the  $2\sigma$  level; all others are at  $1\sigma$ .

collisions. The cross-section for single charged slepton production is too small to be investigated at LEP2. The expected final states from single sneutrino production have been listed and a preliminary investigation of the sensitivity to these signals made. In view of the encouraging results derived here, a future experimental analysis to address this possibility is very welcome.

## Acknowledgements

We thank M. Seymour and M. Krämer for very helpful discussions.

## References

- [1] For a recent review on supersymmetry with broken R-parity see H. Dreiner, hep-ph/9707435.
- [2] S. Dimopoulos and L.J. Hall, Phys. Lett. B 207 (1988) 210
- [3] V. Barger, G. F. Giudice and T. Han, Phys. Rev. **D40** (1989) 2987;
- [4] H. Dreiner, S. Lola, published in “Munich/Annecy/Hamburg 1991, Proceedings,  $e^+e^-$  collisions at 500 GeV”; separately in “Searches for New Physics”, contribution to the LEP2 workshop, 1996, hep-ph/9602207; and “Physics with  $e^+e^-$  Linear Colliders”, DESY-97-100, hep-ph/9705442.
- [5] M. Acciarri et. al., L3 Collaboration, CERN-PPE/97-98, submitted to Phys. Lett. B.; Y. Arnoud et. al., DELPHI Collaboration, “Search for R-Parity violating effects at  $\sqrt{s}$  161 and 172 GeV”, EPS-589, contribution to the EPS-HEP97 conference, Jerusalem.
- [6] J. Erler, J.L. Feng and N. Polonsky, Phys. Rev. Lett. **78** (1997) 3063.
- [7] J. Kalinowski, R. Ruckl, H. Spiesberger, P.M. Zerwas, DESY-97-044, hep-ph/9703436.
- [8] S. Dimopoulos, R. Esmailzadeh, L. J. Hall, G. D. Starkman, Phys. Rev. D 41 (1990) 2099; H. Dreiner, G.G. Ross, Nucl. Phys. B 365 (1991) 597; D.P. Roy, Phys. Lett. B 283 (1992) 270; J. Kalinowski, R. Ruckl, H. Spiesberger, P.M. Zerwas, hep-ph/9708272.
- [9] C.F. Weizsäcker, Z. Phys. **88** (1934) 612; E.J. Williams, Phys. Rev. **45** (1934) 729
- [10] B.C. Allanach et. al., RAL-TR-97-037, hep-ph/9708250.
- [11] S. Frixione et. al. Phys. Lett. **B319** (1993) 339

- [12] T. Sjöstrand, *Comp. Phys. Comm.* **82** (1994) 74
- [13] E. Barberio, B. van Eijk and Z. Was, *Comp. Phys. Comm.* **66** (1991) 115
- [14] J.A.M Vermaseren in “Proceedings of the IVth International Workshop on Gamma Gamma Interactions”, Eds. G. Cochard and P. Kessler, Springer Verlag, 1980.
- [15] R. Barate et. al., ALEPH collaboration, ”Searches for R-parity violating Supersymmetry at LEP II”, EPS-621, contribution to the EPS-HEP97 conference, Jerusalem.
- [16] For reviews of bounds on R-parity violating Yukawa couplings see [1] and G. Bhattacharyya, *Nucl. Phys. Proc. Suppl.* **52A** (1997) 83.